Optical axis perturbation in folded planar ring resonators

Jie Yuan,* Xingwu Long, Bin Zhang, Fei Wang, and Hongchang Zhao

Department of Optoelectronic Engineering, College of Optoelectronic Science and Engineering, National University of Defence Technology, Changsha 410073, China

*Corresponding author: jieyuan@nudt.edu.cn

Received 2 April 2007; revised 4 June 2007; accepted 13 July 2007; posted 19 July 2007 (Doc. ID 80704); published 24 August 2007

A mathematical model of a four-sided folded planar ring resonator is established. The model can be modified into a triangular ring resonator, a square ring resonator, and a four-sided folded ring resonator, all of which are widely used for ring laser gyroscopes by changing certain design parameters such as incident angle Ai and side ratio H. By use of the extended matrix formulation, the optical axis perturbation, including optical axis decentration and optical axis tilt, in those planar ring resonators is analyzed in detail resulting in some novel findings. It has been determined that the longer the mirror radius, the larger the mode volume, the higher the sensitivity of optical axis decentration and the lower the sensitivity of optical axis tilt. The same mirror misalignment value, mostly the misalignment induced by optical axis decentration in the x and y components, has the conventional ratio of $1{:}[\cos(Ai)]^2$ for the symmetrical points of the resonator. Details of the effect of Ai and H on the optical axis tilt have also been determined. The difference in optical axis tilt between different kinds of ring resonator is disclosed. The sensitivity of optical axis tilt was found to undergo singular rapid change along with the right edge of the second stable area. This singular behavior is useful for those resonators that have a small incident angle, such as $Ai = 15°$, because those resonators have a second stable region. These interesting findings are important for cavity design, cavity improvement, and alignment of planar ring resonators.

OCIS codes: 140.3410, 140.3370, 140.3560, 140.4780.

1. Introduction

One of the many successful uses of a laser is as a rotation sensor [1]. There have been many kinds of planar ring resonators that are widely used for laser gyroscopes, including a triangular ring resonator, a square ring resonator, and a four-sided folded ring resonator [1,2]. A ring resonator can also be used to test fundamental physics and geophysics [3]. An overview of ring resonators has been given by Siegman [4]. The research on optical axis perturbation of those ring resonators is useful for cavity design, cavity improvement, and alignment of planar ring resonators.

There has been extensive research on mirror misalignment-induced optical axis perturbation of planar or nonplanar ring resonators [5–14]. For example, nonplanar rings have modified misalignment or optical axis stability properties as analyzed by several authors [5–9]. Optical axis perturbation of ring resonators has also been discussed in Refs. [10–14]. To the best of our knowledge, optical axis perturbation of a four-sided folded planar ring resonator has not yet been analyzed. This four-sided folded planar ring resonator, shown in Figs. 1 and 2, will be illustrated in detail in the following sections. Most of the above-referenced articles are concerned only with one kind of ring resonator and only optical axis decentration. Moreover, most of the previous articles concentrated on the optical axis perturbation of the terminal points of a resonator, where reflective mirrors are located. Actually, the diaphragm of a resonator is not at the terminal points in most cases but at the symmetrical points of the resonator, where there is a minimum spot size. The optical axis perturbation at those symmetrical points needs special attention. For example, when the optical axis of a resonator has an inclined angle with the longitudinal axis of the diaphragm [15], the optical axis passes through the diaphragm under different kinds of optical axis per-

0003-6935/07/256314-09$15.00/0

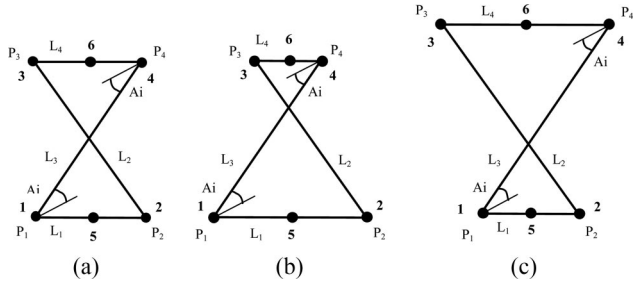

Fig. 1. Four-sided folded planar ring cavity used for the analysis with (a) $H = 1$; (b) $H < 1$; (c) $H > 1$; 1, 2, curved mirror; 3, 4, plane mirror; Ai, incident angle.

turbation, as shown in Fig. 3. After optical axis decentration, the optical axis passes through the center of the diaphragm but the inclined angle still exists; see Fig. 3(a). After optical axis tilt, the optical axis is parallel to the longitudinal axis of the diaphragm but does not pass through the center of the diaphragm; see Fig. 3(b). After optical axis decentration and tilt, the optical axis is not only to parallel to the longitudinal axis of the diaphragm but it also passes through the center of the diaphragm; see Fig. 3(c). In other words, the optical axis decentration can cause the optical axis to pass through the center of the diaphragm, and the optical axis tilt can cause the optical axis to be parallel to the longitudinal axis. If the mirror misalignment-induced optical axis tilt is sensitive, the inclined angle of the optical axis can easily be modified and the optical axis can be parallel to the longitudinal axis by adjustment of the azimuthal angle of the planar or spherical mirrors of a ring resonator. If the optical axis tilt is not sensitive, it would be difficult for the optical axis to be parallel to the longitudinal axis. The sensitivity of the optical axis tilt is also important for cavity design and alignment of resonators.

We establish a mathematical model of a four-sided folded planar ring resonator. The model can be modified as a triangular resonator, a square ring resonator, and a four-sided folded ring resonator by changing the incident angle and the side ratio. Such ring resonators are widely used for ring laser gyroscopes. By use of an extended matrix formulation, the optical axis decentration and especially the optical axis tilt will be analyzed in detail. Several symmetrical points in the resonator will also be discussed in detail. The optical axis perturbations of different kinds of planar ring resonator will be compared, and the effects of different design parameters on optical axis perturbation will be investigated in depth.

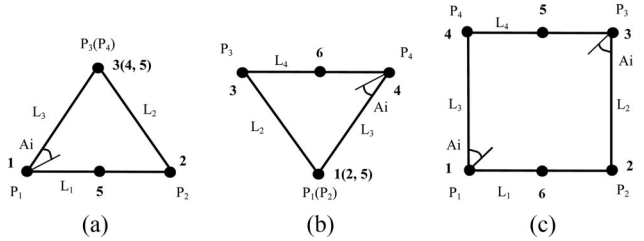

Fig. 2. Several special cases of a four-sided folded planar ring cavity: (a) regular triangular ring cavity with $H = 0$, $Ai = 30°$, and $L_1 = L_2 = L_3$; (b) regular triangular ring cavity with $H = \infty$, $Ai = 30°$, and $L_2 = L_3 = L_4$; (c) square ring cavity with $Ai = 45°$ and $L_1 = L_2 = L_3 = L_4$.

2. Analytical Method

As shown in Figs. 1 and 2, we analyze the four-sided folded planar ring cavity. Mirrors P_1 and P_2 are spherical mirrors with a common radius R; mirrors P_3 and P_4 were chosen to be flat. Points 1, 2, 3, and 4 are the terminal points of the resonator. Points 5 and 6 are the midpoints between two curved mirrors, P_1 and P_2, and the midpoints between the two flat mirrors, P_3 and P_4. The total cavity length is L, and $L = L_1 + L_2 + L_3 + L_4$. H is defined as the side ratio of L_4 and L_1, and $H = L_4/L_1$. The incident angles for all four mirrors are equal to Ai, and Ai can be varied from 0° to 45°. If L, Ai, and H are independent variables, the length of the four sides can be written as

$$L_1 = \frac{L}{(1+H)[1+1/\cos(2Ai)]}, \tag{1}$$

$$L_4 = L_1 H = \frac{LH}{(1+H)[1+1/\cos(2Ai)]}, \tag{2}$$

$$L_2 = L_3 = \frac{(L_1+L_4)}{2\cos(2Ai)} = \frac{1}{2}\frac{L}{\cos(2Ai)+1}. \tag{3}$$

There are many special cases of four-sided folded planar ring resonators, as shown in Figs. 1(a)–1(c) with $H = 1$, $H < 1$, and $H > 1$, respectively, i.e., $L_4 = L_1$, $L_4 < L_1$, and $L_4 > L_1$. When $H = 0$ or $H = \infty$, $L_4 = 0$ or $L_1 = 0$, and the four-sided folded planar ring resonators are changed into triangular ring resonators having two spherical mirrors or two flat mirrors. The triangular ring resonators are shown in Figs. 2(a) and 2(b). If $Ai = 30°$, the above-mentioned two kinds of triangular ring resonator are regular triangles. When $Ai = 45°$ and $L_1 = L_2 = L_3 = L_4$, the four-sided planar ring cavity becomes a square ring cavity, as shown in Fig. 2(c). All the special cases can be used for ring laser gyroscopes.

To investigate the optical axis behavior of a four-sided folded planar ring cavity and its special cases as shown in Figs. 1 and 2, it is necessary to determine the general round-trip propagation ray matrix that includes the perturbation of its optical components. Ray optics with misaligned elements and extended matrix formulation was presented by Siegman [15] and by Gerrard and Burch [16]. For the resonators that we consider, it is convenient to include the capability to treat tilt in two orthogonal planes simultaneously. So we apply the extended 5×5 ray matrices [10,11,15]. The ray matrix of a general optical component with angular misalignment has the form

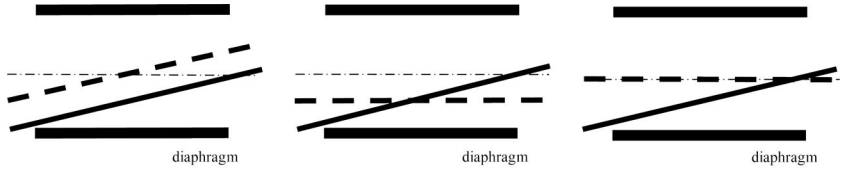

Fig. 3. Schematic diagram of an optical-axis as it passes through the diaphragm under different kinds of optical axis perturbation such as (a) decentration, (b) tilt, (c) decentration and tilt. The center line represents the longitudinal axis of the diaphragm; the solid and broken lines represent the optical axis before and after perturbation.

$$\begin{pmatrix} r_{ox} \\ r_{ox}' \\ r_{oy} \\ r_{oy}' \\ 1 \end{pmatrix} = \begin{pmatrix} A_x & B_x & 0 & 0 & 0 \\ C_x & D_x & 0 & 0 & \xi_x \\ 0 & 0 & A_y & B_y & 0 \\ 0 & 0 & C_y & D_y & \xi_y \\ 0 & 0 & 0 & 0 & 1 \end{pmatrix} \begin{pmatrix} r_{ix} \\ r_{ix}' \\ r_{iy} \\ r_{iy}' \\ 1 \end{pmatrix}, \tag{4}$$

where r_{ix}, r_{iy}, r_{ox}, and r_{oy} are the input ray and the output ray heights from the reference axis along the x and y axes, respectively, which we call optical axis decentration. r_{ix}', r_{iy}', r_{ox}', and r_{oy}' are the angles that the input ray and the output ray make with the reference axis in the x and y planes, respectively, which we call optical axis tilt. A_x, B_x, C_x, and D_x are standard ray matrix elements in the tangential plane; A_y, B_y, C_y, and D_y are standard ray matrix elements in the sagittal plane; and ξ_x and ξ_y are the angular perturbations induced by the optical component. In the case of a mirror, $\xi_x = 2\tan(\theta_x)$ $\xi_y = 2\tan(\theta_y)$, θ_x and θ_y are the misalignment angles of the mirror in its local tangential and sagittal planes, respectively. Here we focus the mirror misalignment on the main source of perturbation. The ray matrix of a reflective mirror P_i with angular misalignment as a perturbation source can be expressed as

$$M(P_i) = \begin{bmatrix} 1 & 0 & 0 & 0 & 0 \\ -\dfrac{2}{R_i \times \cos Ai} & 1 & 0 & 0 & 2\theta_{xi} \\ 0 & 0 & 1 & 0 & 0 \\ 0 & 0 & -\dfrac{2 \times \cos Ai}{R_i} & 1 & 2\theta_{yi} \\ 0 & 0 & 0 & 0 & 1 \end{bmatrix}. \tag{5}$$

The ray matrix of free-space propagation L is given by

$$M(L) = 0\begin{bmatrix} 1 & L & 0 & 0 & 0 \\ 0 & 1 & 0 & 0 & 0 \\ 0 & 0 & 1 & L & 0 \\ 0 & 0 & 0 & 1 & 0 \\ 0 & 0 & 0 & 0 & 1 \end{bmatrix}. \tag{6}$$

The ray matrix for round-trip propagation in a resonator is the product of each individual matrix in proper sequential order:

$$M = \prod M_i. \tag{7}$$

The location of the optical axis is given by the eigenvector corresponding to eigenvalue 1. At this time the resonator optical axis is invariant under the round-trip propagation:

$$\begin{pmatrix} r_x \\ r_x' \\ r_y \\ r_y' \\ 1 \end{pmatrix} = M \begin{pmatrix} r_x \\ r_x' \\ r_y \\ r_y' \\ 1 \end{pmatrix}. \tag{8}$$

Equation (8) can be simplified as

$$\begin{bmatrix} M11-1 & M12 & M13 & M14 \\ M21 & M22-1 & M23 & M24 \\ M31 & M32 & M33-1 & M34 \\ M41 & M42 & M43 & M44-1 \end{bmatrix} \times \begin{bmatrix} r_x \\ r_x' \\ r_y \\ r_y' \end{bmatrix} = -\begin{bmatrix} M15 \\ M25 \\ M35 \\ M45 \end{bmatrix}. \tag{9}$$

The optical axis location (r_x, r_y) and slope (r_x', r_y') under the influence of any component misalignment or optical axis decentration and tilt can be found by solving Eq. (9). Here we introduce the following two dimensionless sensitivity factors:

$$\mathrm{SD}_{\left(\frac{x}{y}\right)i\left(\frac{x}{y}\right)j} = \frac{1}{L}\left[\frac{\partial r_{\left(\frac{x}{y}\right)i}}{\partial \theta_{\left(\frac{x}{y}\right)j}}\right], \tag{10}$$

$$\mathrm{ST}_{\left(\frac{x}{y}\right)i\left(\frac{x}{y}\right)j} = \frac{1}{L}\left[\frac{\partial r'_{\left(\frac{x}{y}\right)i}}{\partial \theta_{\left(\frac{x}{y}\right)j}}\right], \tag{11}$$

where

$$r_{\left(\frac{x}{y}\right)i}, \qquad r'_{\left(\frac{x}{y}\right)i}$$

are the induced x or y component of optical axis decentration and optical axis tilt on the ith mirror as the result of the jth mirror tangential or sagittal direction angular misalignment of an amount $\theta_{\left(\frac{x}{y}\right)j}$ (in radians). That is to say, we use SD and ST to describe the sensitivity of optical axis decentration and the sensitivity of optical axis tilt, respectively. If the value of SD increases, the optical axis on point i will allow for easier adjustment of optical axis decentration by applying the misalignment of the jth mirror. Similarly, if the value of ST increases, the optical

axis on point i will allow for easier adjustment of the optical axis tilt by applying the misalignment of the jth mirror. In contrast, if the values decrease, the adjustments will be more difficult.

The source of perturbation in this analysis is the misalignment of spherical mirrors P_1 and P_2, or planar mirrors P_3 and P_4 in there local tangential and sagittal planes. Special symmetrical points 5 and 6 were chosen for discussion for the following sections.

For a planar ring resonator, the stability function is $(A + D/2)$ and the stability condition is [15,17,18]

$$-1 < (A + D/2) < 1, \tag{12}$$

where A and D are the matrix elements of the overall $ABCD$ matrix that can be obtained by multiplying the $ABCD$ matrices of the elementary components. For a ring resonator that has two nonequivalent orthogonal planes of meridian symmetry, the $ABCD$ matrix problem must be solved independently in the two orthogonal transverse x and y directions and the stability condition should be satisfied simultaneously in the x and y directions for a stable ring resonator. A stable ring resonator means that the radial coordinate at amplitude e^{-1} in the x and y directions is finite.

3. Numerical Analysis Results

A. Optical Axis Decentration

Considering the two special points 5 and 6, the following results can be obtained by solving Eq. (9):

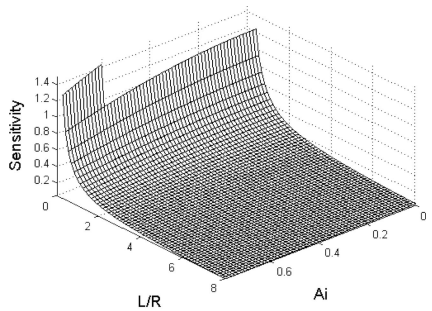

(a)

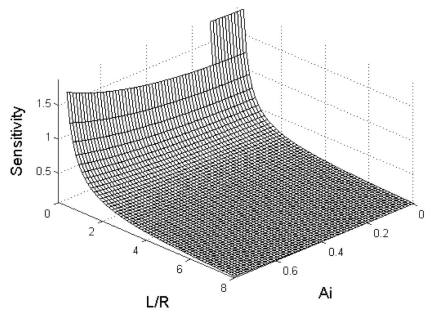

(b)

Fig. 4. Sensitivity of optical axis decentration versus L/R and Ai: (a) $SD_{x_5x_1}$ and (b) $SD_{y_5y_1}$.

$$SD_{x_5x_1} = SD_{x_6x_1} = SD_{x_5x_3} = \frac{1}{2}\frac{\cos(Ai)}{L/R}, \tag{13}$$

$$SD_{y_5y_1} = SD_{y_6y_1} = SD_{y_5y_3} = \frac{1}{2}\frac{1}{(L/R)\cos(Ai)}, \tag{14}$$

$$SD_{x_6x_3} = -\frac{1}{2}\frac{[L/R - \cos(Ai) - \cos(Ai)\cos(2Ai)]}{(L/R)[\cos(2Ai) + 1]}, \tag{15}$$

$$SD_{y_6y_3} = -\frac{1}{2}\frac{[(L/R)\cos(Ai) - 1 - \cos(2Ai)]}{(L/R)(\cos(2Ai) + 1)\cos(Ai)}. \tag{16}$$

It has been determined that, with an increase in L/R, the misalignment induced in mirrors P_1 and P_2 by optical axis decentration under points 5 and 6 including the x and y components both decrease. All the sensitivity of optical axis decentration is invariant when H varies. With an increase in Ai, the optical axis movement $SD_{y_iy_j}$ increases and $SD_{x_ix_j}$ decreases, where i ranges from 5 to 6 and j ranges from 1 to 4. $SD_{x_5x_1}$ and $SD_{y_5y_1}$ were chosen as examples and are shown in Fig. 4.

One can easily obtain the following results by comparing the values in Eqs. (13) and (14):

$$\frac{SD_{y_5y_1}}{SD_{x_5x_1}} = \frac{SD_{y_6y_1}}{SD_{x_6x_1}} = \frac{SD_{y_5y_3}}{SD_{x_5x_3}} = \frac{1}{[\cos(Ai)]^2}. \tag{17}$$

That is to say, for the same mirror misalignment, the misalignment induced by optical axis decentration in

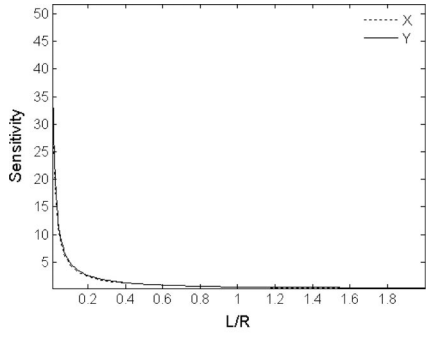

(a)

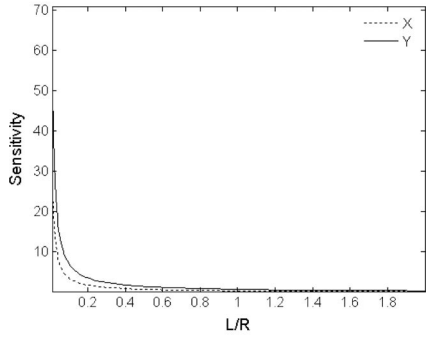

(b)

Fig. 5. Sensitivity of optical axis decentration versus L/R with different incident angles: (a) $Ai = 15°$ and (b) $Ai = 45°$. Solid curve, the value of the y component including $SD_{y_5y_1}$ and $SD_{y_6y_1}$; dashed curve, the value of the x component including $SD_{x_5x_1}$ and $SD_{x_6x_1}$.

the x and y components has the common ratio of $1{:}[\cos(Ai)]^2$ for points 5 and 6 except for the ratio of $SD_{y_6y_3}/SD_{x_6x_3}$. When incident angle Ai is 22.5, 30, or 45 deg, the ratio would be 1.172, 1.333, and 2, respectively. $SD_{x_5x_1}$, $SD_{x_6x_1}$, $SD_{y_5y_1}$, and $SD_{y_6y_1}$ were chosen as examples and are shown in Fig. 5. $Ai = 45°$ corresponds to the resonator shown in Fig. 2(c). Obviously the ratio between the y component and the x component under the condition of $Ai = 45°$ is greater than that of $Ai = 15°$. This characteristic does not change with the variation of H. That is to say, all the resonators shown in Figs. 1 and 2 have the same characteristic.

B. Optical Axis Tilt

First, we would like to determine the effect of incident angle Ai and L/R on the optical axis tilt. The following results were determined for the two special symmetrical points 5 and 6:

(1) With an increase in L/R, the absolute value of the sensitivity of the optical axis tilt induced by the misalignment of mirrors P_1 and P_2 or P_3 and P_4 will also increase if the resonator is a folded four-sided ring resonator with a different value for Ai, a triangular ring resonator, or a square ring resonator. This is contrary to the behavior of optical axis decentration sensitivity.

(2) With the increase of Ai, the absolute value of the sensitivity of the optical axis tilt under the location of point 5 induced by the misalignment of P_1 and P_2 also increases in most cases, whereas the value of point 6 induced by the misalignment of P_1 and P_2 decreases. An exception occurred for $ST_{x_5x_1}$, as shown in Fig. 6(c).

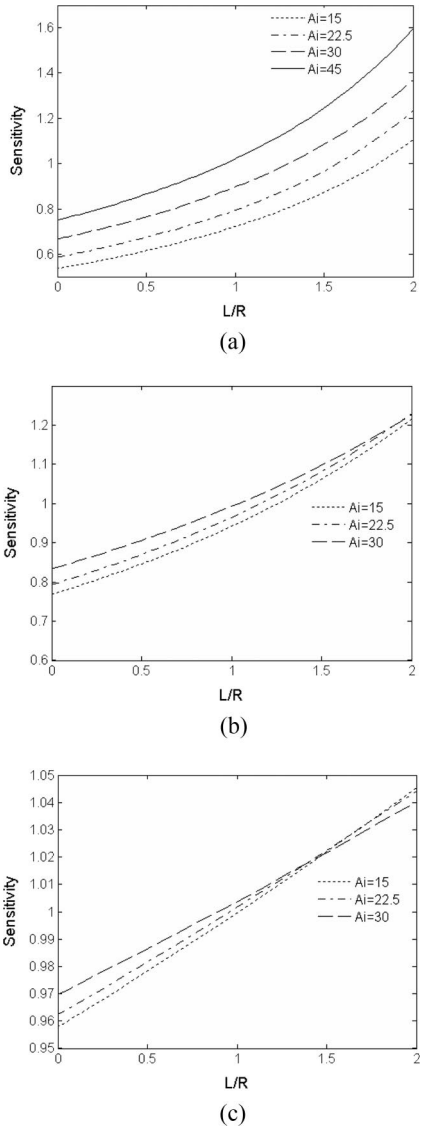

Fig. 6. Sensitivity of optical axis tilt $ST_{x_5x_1}$ with incident angles of 15, 22.5, 30, and 45 deg versus L/R and with different values for H: (a) $H = 0$, (b) $H = 1$, (c) $H = 10$.

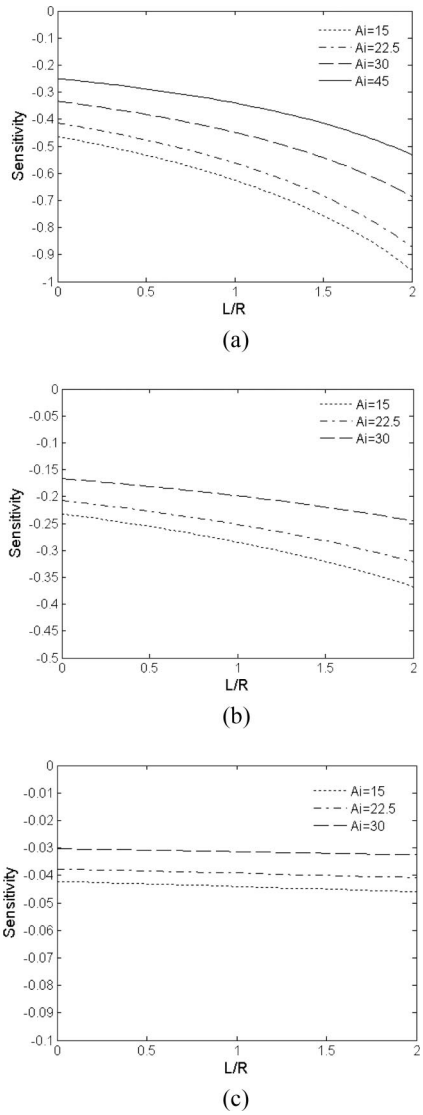

Fig. 7. Sensitivity of optical axis tilt $ST_{x_6x_1}$ with incident angles of 15, 22.5, 30, and 45 deg versus L/R and with different values for H: (a) $H = 0$, (b) $H = 1$, (c) $H = 10$.

(3) With the increase of Ai, the absolute value of the sensitivity of the optical axis tilt under the location of point 5 induced by the misalignment of planar mirrors P_3 and P_4 decreases, whereas the value of point 6 induced by the misalignment of P_3 and P_4 increases. $ST_{x_5x_1}$, $ST_{x_6x_1}$, $ST_{x_5x_3}$, and $ST_{x_6x_3}$ were chosen as examples and are shown in Figs. 6, 7, 8, and 9, respectively.

Second, we wish to determine the effect of side ratio H on the optical axis tilt. The following results were determined for the two special symmetrical points 5 and 6. With an increase in H, the absolute value of the sensitivity of the optical axis tilt under the location of point 5 induced by the misalignment of spherical mirrors P_1 and P_2 or planar mirrors P_3 and P_4 increased in most cases, whereas the absolute value of point 6 induced by the misalignment of P_1 and P_2 or P_3 and P_4 decreased in most cases. $ST_{x_5x_1}$, $ST_{x_6x_1}$, $ST_{x_5x_3}$, and $ST_{x_6x_3}$ were chosen as examples and are shown in Figs. 10 and 11, respectively. An exception occurred for $ST_{x_5x_1}$, as shown in Fig. 10(a).

Third, the above results were all obtained under the condition of $0 < L/R < 2$. For all the folded planar ring lasers mentioned above, a stable region exists inside the region of $0 < L/R < 2$, which we call the first stable region. When $2 < L/R < \infty$, for some big values of Ai such as 22.5, 30, or 45 deg, the second stable region of the x and y components does not have any overlap area. That is to say, the resonator does not really have a second stable region. For some small values of Ai such as 15°, the second stable region of the x and y components does have an overlap area. That is to say, the resonator does have a second stable region.

The sensitivity of optical axis decentration and optical axis tilt including $SD_{x_5x_1}$, $SD_{y_5y_1}$, $ST_{x_5x_1}$, and $ST_{y_5y_1}$

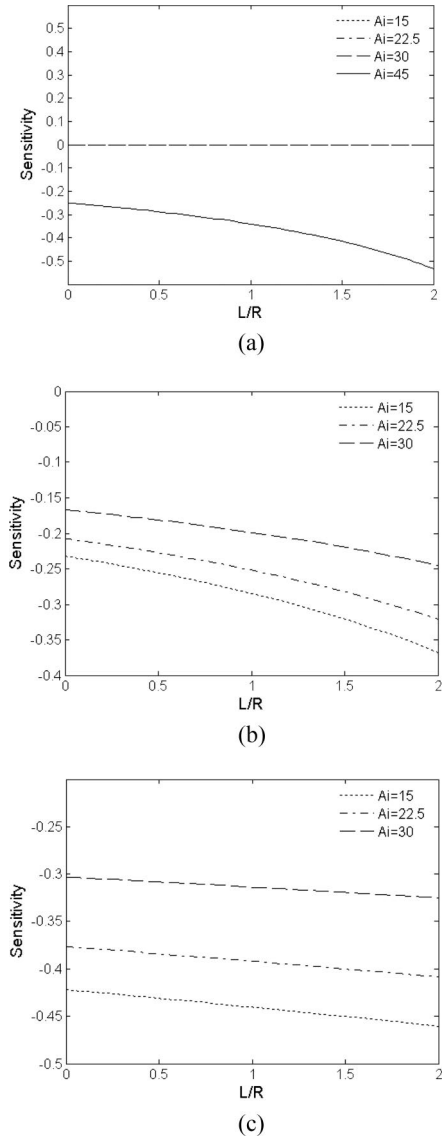

Fig. 8. Sensitivity of optical axis tilt $ST_{x_5x_3}$ with incident angles of 15, 22.5, 30, and 45 deg versus L/R and with different values for H: (a) $H = 0$, (b) $H = 1$, (c) $H = 10$.

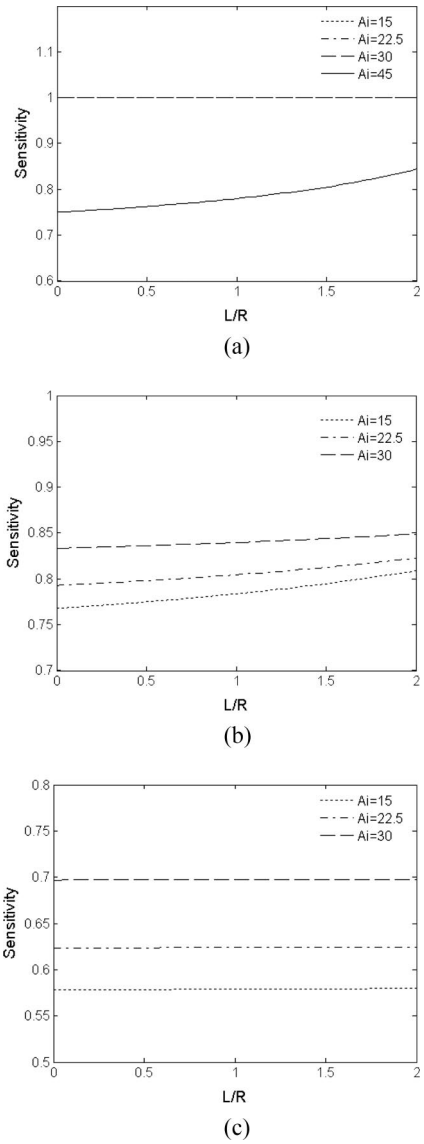

Fig. 9. Sensitivity of optical axis tilt $ST_{x_6x_3}$ with incident angles of 15, 22.5, 30, and 45 deg versus L/R and with different values for H: (a) $H = 0$, (b) $H = 1$, (c) $H = 10$.

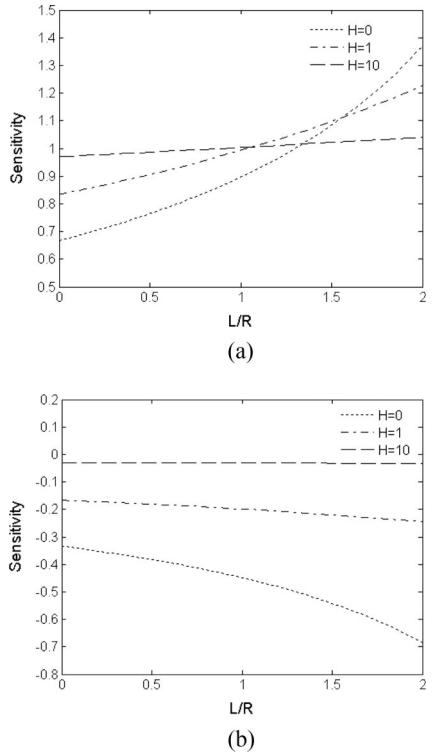

Fig. 10. Sensitivity of optical axis tilt with $H = 0$, 1, and 10 and $Ai = 30°$ versus L/R: (a) $ST_{x_5x_1}$ and (b) $ST_{x_6x_1}$.

versus L/R was chosen as an example and each is shown in Figs. 12 and 13 for $H = 1, Ai = 30°$, and 15°. The stability criteria $(A + D/2)$ at both the x and the

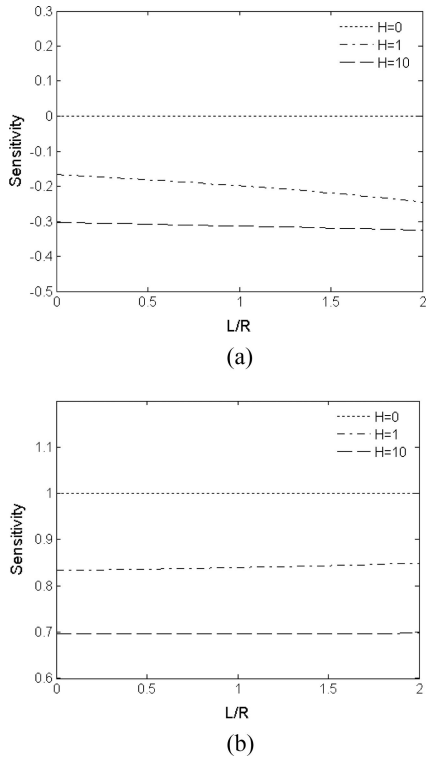

Fig. 11. Sensitivity of optical axis tilt with $H = 0$, 1, and 10 and $Ai = 30°$ versus L/R: (a) $ST_{x_5x_3}$ and (b) $ST_{x_6x_3}$.

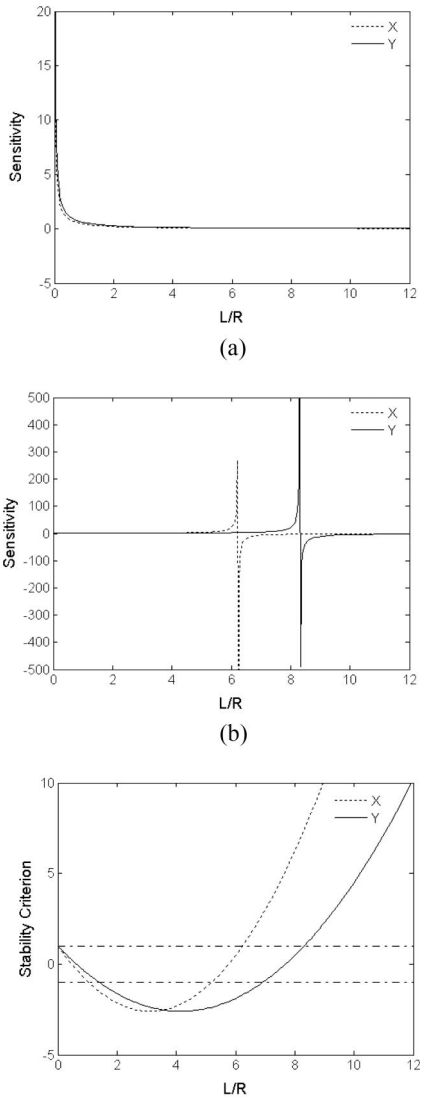

Fig. 12. (a) Sensitivity of optical axis decentration including $SD_{x_5x_1}$ (broken curve) and $SD_{y_5y_1}$ (solid curve) versus L/R. (b) Sensitivity of optical axis tilt including $ST_{x_5x_1}$ (broken curve) and $ST_{y_5y_1}$ (solid curve) versus L/R. (c) The stability function $(A + D/2)$ in both the x and the y directions of the ring resonator versus L/R. $H = 1, Ai = 30°$, and L/R ranges from 0 to 12. The dash–dot lines in (c) represent the critical values of -1 and 1.

y directions of the ring resonator versus L/R are shown in Figs. 12(c) and 13(c) for $H = 1$ and $Ai = 30°$ and 15°. When $Ai = 30°$, as shown in Fig. 12, the first stable region is $0 < L/R < 0.744$, that is to say, the stability function $(A + D/2)$ is between the critical value of -1 and 1 in the region of $0 < L/R < 0.744$. No second stable region exists inside the region of $2 < L/R < \infty$. When $Ai = 15°$, as shown in Fig. 13, the first stable region is $0 < L/R < 1.008$ and the second stable region is $4.45 < L/R < 5.39$.

As shown in Figs. 12 and 13, the sensitivity of the optical axis decentration does not have any singularity inside the whole region of $0 < L/R < \infty$, and the relation between the sensitivity and the L/R obeys

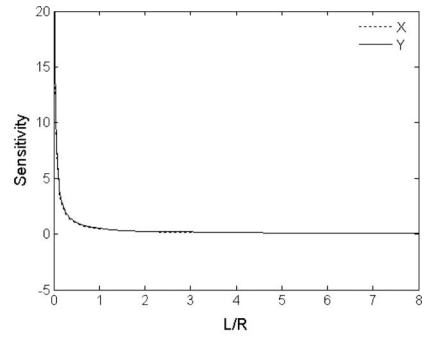

(a)

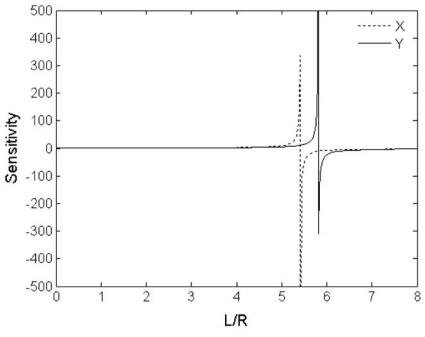

(b)

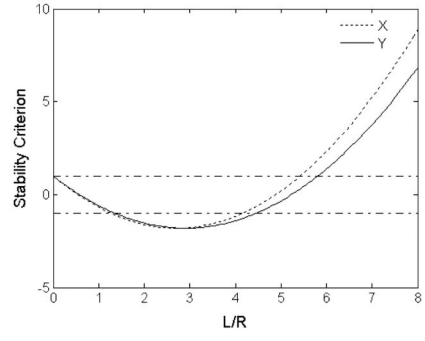

(c)

Fig. 13. (a) Sensitivity of optical axis decentration including $SD_{x_5x_1}$ (broken curve) and $SD_{y_5y_1}$ (solid curve) versus L/R. (b) Sensitivity of optical axis tilt including $ST_{x_5x_1}$ (broken curve) and $ST_{y_5y_1}$ (solid curve) versus L/R. (c) The stability function $(A + D/2)$ in both the x and the y directions of the ring resonator versus L/R. $H = 1, Ai = 15°, L/R$ ranges from 0 to 8. The dash–dot lines in (c) represent the critical values of -1 and 1.

the rules mentioned above: the longer the mirror radius, the larger the mode volume and the higher the sensitivity of optical axis decentration. The sensitivity of optical axis tilt does not have any **singularity** inside the first stable region. The relation between the sensitivity and the L/R is opposite that of optical axis decentration: the longer the mirror radius, the larger the mode volume and the lower the sensitivity of the optical axis tilt. When the value of L/R ranges from 2 to ∞, the sensitivity of the optical axis tilt was found to have an instability point at a certain value of L/R for all the points inside the ring optical path including points 1, 2, 3, 4, 5, and 6 as shown in Figs. 1 and 2. This specific value of L/R is located at the right edge of the second stable region within the area of $2 < L/R < \infty$. The sensitivity of the optical axis tilt at the x and y components was found to have a singular rapid change along the right edge of the second stable area within the area of $2 < L/R < \infty$. This singular behavior is useful for those resonators with small incident angle values such as $Ai = 15°$ because those resonators do have a second stable region.

4. Conclusion

For the four-sided folded planar ring resonators and its special cases including triangular and square ring resonators, we determined that the longer the mirror radius, the larger the mode volume, the higher the sensitivity of optical axis decentration and the lower the sensitivity of optical axis tilt. For the same mirror misalignment, that induced by optical axis decentration in the x and y components has the common ratio of $1:[\cos(Ai)]^2$ for symmetrical points 5 and 6 except for the ratio of $SD_{y_6y_3}/SD_{x_6x_3}$. The effect of incident angle Ai and side ratio H on the optical axis tilt has also been determined in detail. That is to say, the difference in optical axis tilt between different kinds of ring resonator has been disclosed. Sensitivity of the optical axis tilt was found to have a singular rapid change along with the right edge of the second stable area within the area of $2 < L/R < \infty$. This singular behavior is useful for those resonators that have a small value of incident angle such as $Ai = 15°$ because the resonators do have a second stable region.

This research was supported by the National Science Foundation of China under grant 60608002.

References

1. W. W. Chow, J. Gea-Banacloche, L. M. Pedrotti, V. E. Sanders, W. Schleich, and M. O. Scully, "The ring laser gyro," Rev. Mod. Phys. **57,** 61–86 (1985).
2. K. Andringa, "Laser gyroscope," U. S. patent 3,741,657 (26 June 1973).
3. G. E. Stedman, "Ring-laser tests of fundamental physics and geophysics," Rep. Prog. Phys. **60,** 615–688 (1997).
4. A. E. Siegman, "Laser beams and resonators: the 1960s," IEEE J. Special Top. Quantum Electron. **20,** 100–110 (1999).
5. J. A. Arnaud, "Degenerate optical cavities. II. Effect of misalignments," Appl. Opt. **8,** 1909–1917 (1969).
6. G. B. Altshuler, E. D. Isyanova, V. B. Karasev, A. L. Levit, V. M. Ovchinnikov, and S. F. Sharlai, "Analysis of misalignment sensitivity of ring laser resonators," Sov. J. Quantum Electron. **7,** 857–859 (1977).
7. I. W. Smith, "Optical resonator axis stability and instability from first principles," in *Fiber Optic and Laser Sensors I,* E. L. Moore and O. G. Ramer, eds., Proc. SPIE **412,** 203–206 (1983).
8. A. L. Levit and V. M. Ovchinnikov, "Stability of a ring resonator with a nonplane axial contour," J. Appl. Spectrosc. (USSR) **40,** 657–660 (1984).
9. S. C. Sheng, "Optical-axis perturbation singularity in an out-of-plane ring resonator," Opt. Lett. **19,** 683–685 (1994).
10. A. H. Paxton and W. H. Latham, Jr., "Ray matrix method for the analysis of optical resonators with image rotation," in *1985 International Lens Design Conference,* D. T. Moore and W. H. Taylor, eds., Proc. SPIE **554,** 159–163 (1985).
11. A. H. Paxton and W. P. Latham, Jr., "Unstable resonators with 90° beam rotation," Appl. Opt. **25,** 2939–2946 (1986).

12. R. Rodloff, "A laser gyro with optimized resonator geometry," IEEE J. Quantum Electron. **QE-23,** 438–445 (1987).
13. H. R. Bilger and G. E. Stedman, "Stability of planar ring lasers with mirror misalignment," Appl. Opt. **26,** 3710–3716 (1987).
14. M. L. Stitch and M. Bass, eds., *Laser Handbook* (North-Holland, 1985), Vol. 4, Chap. 3, pp. 229–332.
15. A. E. Siegman, *Lasers* (University Science, 1986), Chap. 15.
16. A. Gerrard and J. M. Burch, *Introduction of Matrix Methods in Optics* (Wiley, 1975).
17. O. Svelto, *Principles of Lasers,* 4th ed. (Springer, 1998), translated by D. C. Hanna.
18. J. Yuan, X. W. Long, L. M. Liang, B. Zhang, F. Wang, and H. C. Zhao, "Nonplanar ring resonator modes: generalized Gaussian beams," Appl. Opt. **46,** 2980–2989 (2007).